

The formation efficiency of close-in planets via Lidov-Kozai migration: analytic calculations

Diego J. Muñoz^{1*}, Dong Lai¹ and Bin Liu²

¹ *Cornell Center for Astrophysics and Planetary Science, Department of Astronomy, Cornell University, Ithaca, NY 14853, USA*

² *Center for Astrophysics, University of Science and Technology of China, Hefei, Anhui 230026, People's Republic of China*

25 January 2016

ABSTRACT

Lidov-Kozai oscillations of planets in stellar binaries, combined with tidal dissipation, can lead to the formation of hot Jupiters (HJs) or tidal disruption of planets. Recent population synthesis studies have found that the fraction of systems resulting in HJs (\mathcal{F}_{HJ}) depends strongly on the planet mass, host stellar type and tidal dissipation strength, while the total migration fraction $\mathcal{F}_{\text{mig}} = \mathcal{F}_{\text{HJ}} + \mathcal{F}_{\text{dis}}$ (including both HJ formation and tidal disruption) exhibits much weaker dependence. We present an analytical method for calculating \mathcal{F}_{HJ} and \mathcal{F}_{mig} in the Lidov-Kozai migration scenario. The key ingredient of our method is to determine the critical initial planet-binary inclination angle that drives the planet to reach sufficiently large eccentricity for efficient tidal dissipation or disruption. This calculation includes the effects of octupole potential and short-range forces on the planet. Our analytical method reproduces the resulting planet migration/disruption fractions from population synthesis, and can be easily implemented for various planet, stellar/companion types, and for different distributions of initial planetary semi-major axes, binary separations and eccentricities. We extend our calculations to planets in the super-Earth mass range and discuss the conditions for such planets to survive Lidov-Kozai migration and form close-in rocky planets.

Key words: binaries:general – planets: dynamical evolution and stability – star: planetary system

1 INTRODUCTION

The occurrence of “hot Jupiters” (HJs) – gas giants with periods $\lesssim 5$ days – is estimated to be around 1% for FGK stars (Marcy et al. 2005; Wright et al. 2012; Howard et al. 2012; Fressin et al. 2013; Petigura, Howard & Marcy 2013). It is commonly believed that these planets formed at larger separations from their host stars (presumably beyond the ice line) and subsequently “migrated” to semi-major axes of less than 0.1 AU. The known migration mechanisms can be (i) “disc mediated” due to planet-disc interaction (e.g., Goldreich & Tremaine 1980; Lin, Bodenheimer & Richardson 1996), (ii) “planet mediated”, including strong planet-planet scatterings and various forms of secular interactions among multiple planets (e.g. Rasio & Ford 1996; Chatterjee et al. 2008; Jurić & Tremaine 2008; Nagasawa, Ida & Bessho 2008; Wu & Lithwick 2011; Beaugé & Nesvorný 2012; Petrovich 2015a), or (iii) “binary mediated”, i.e., secular interactions with a distant stellar companion (Wu & Murray 2003; Wu, Murray & Ramsahai 2007; Fabrycky & Tremaine 2007; Naoz, Farr & Rasio 2012; Correia et al. 2011; Storch, Anderson & Lai 2014; Petrovich 2015b; Anderson, Storch & Lai 2016). Excluding disc-driven migration, these mechanisms require the migrating planet to reach high eccentricities in order for

tidal dissipation at pericenter to shrink the planet semi-major axis down to $\lesssim 0.1$ AU. Thus, such mechanisms are sometimes referred to collectively as “high- e migration”.

Planet migration following eccentricity excitation through Lidov-Kozai oscillations (Lidov 1962; Kozai 1962) induced by a stellar companion¹ – often called Lidov-Kozai (LK) migration – has been investigated by different researchers via Monte Carlo experiments (Wu, Murray & Ramsahai 2007; Fabrycky & Tremaine 2007; Naoz, Farr & Rasio 2012; Petrovich 2015b; Anderson, Storch & Lai 2016). The latest studies have concluded that at most 20% of observed HJs can be explained by LK migration in stellar binaries. Similarly, observational evidence (Dawson & Murray-Clay 2013; Dawson, Murray-Clay & Johnson 2015) also indicates that the population of HJs is unlikely to be explained by a single migration mechanism.

The occurrence rate of HJs produced by LK migration in stellar binaries can be computed via

$$\mathcal{R}_{\text{HJ}}^{\text{LK}} = \mathcal{F}_b \times \mathcal{F}_p \times \mathcal{F}_{\text{HJ}}^{\text{LK}}, \quad (1)$$

where \mathcal{F}_b is fraction of stars having a wide binary companion, \mathcal{F}_p is

¹ LK oscillations induced by a planetary companion can play an important role in some planet-mediated high- e migration scenarios. In this paper, we focus on LK oscillations induced by a stellar-mass companion.

* E-mail: dmunoz@astro.cornell.edu

the fraction of solar-type stars hosting a “regular” giant planet at a distance of a few AU, and $\mathcal{F}_{\text{HJ}}^{\text{LK}}$ is the formation fraction/efficiency of HJs (i.e., the fraction of systems that result in HJs for a given distributions of binaries and “regular” planets). Optimistic values of $\mathcal{F}_b \sim 20\%$ (for binary separations between 100 AU and 1000 AU; see Raghavan et al. 2010) and $\mathcal{F}_p \sim 15\%$ (Petrovich 2015b) require $\mathcal{F}_{\text{HJ}}^{\text{LK}} \sim 30\%–40\%$ to explain the observed HJ occurrence rate ($\sim 1\%$) using LK migration alone.

In a recent work, Anderson, Storch & Lai (2016) (hereafter ASL) conducted a comprehensive population synthesis study of HJ formation from LK oscillations in stellar binaries, including all relevant physical effects (the octupole potential from the binary companion, mutual precession of the host stellar spin axis and planet orbital axis, tidal dissipation, and stellar spin-down due to magnetic braking). Unlike previous works, ASL considered a range of planet masses ($0.3–5M_J$) and initial semi-major axes ($a_0 = 1–5$ AU), different properties for the host star, and varying tidal dissipation strengths. They found that the HJ formation efficiency depends strongly on planet mass and stellar type, with $\mathcal{F}_{\text{HJ}}^{\text{LK}} = 1–4\%$ (depending on tidal dissipation strength) for $M_p = 1 M_J$, and larger (up to 8%) for more massive planets. The production efficiency of “hot Saturns” ($M_p = 0.3 M_J$) is much lower, because most migrating planets are tidally disrupted. Remarkably, ASL found that the fraction of migrating systems, i.e. those that result in either HJ formation or tidal disruption, $\mathcal{F}_{\text{mig}}^{\text{LK}} \equiv \mathcal{F}_{\text{HJ}}^{\text{LK}} + \mathcal{F}_{\text{dis}}^{\text{LK}} \simeq 11–14\%$ is roughly constant, having little variation with planet mass, stellar type and tidal dissipation strength. ASL provided a qualitative explanation of how such a robust $\mathcal{F}_{\text{mig}}^{\text{LK}}$ may come about (see Sections 3.4 and 5.4.1 of that work). Note that (Petrovich 2015b) considered $M_p = 1 M_J$ around solar-type stars and found a similar $\mathcal{F}_{\text{HJ}}^{\text{LK}}$ as ASL, but a much larger disruption fraction ($\mathcal{F}_{\text{dis}}^{\text{LK}} \sim 25\%$), and thus obtained $\mathcal{F}_{\text{mig}}^{\text{LK}} \approx 27–29\%$. The difference arises from the fact that (Petrovich 2015b) placed all planets initially at $a_0 = 5$ AU and assumed that the binary eccentricity distribution extends up to 0.95, whereas ASL considered $a_0 = 1–5$ AU and a maximum binary eccentricity of 0.8 (see Section 6.2 of ASL for further discussion).

In this paper, following on the work of ASL, we present an analytic study that explains (i) how the LK migration fraction of close-in planets are largely determined by geometrical considerations, and (ii) how the planet survival and disruption fractions depend on the properties of the planets and host stars. We outline the necessary steps that allow for simple calculations of $\mathcal{F}_{\text{mig}}^{\text{LK}}$, $\mathcal{F}_{\text{HJ}}^{\text{LK}}$ and $\mathcal{F}_{\text{dis}}^{\text{LK}}$ under various conditions and assumptions (e.g., the distributions of initial planetary semi-major axes, binary separations and eccentricities, the masses of planet and host star). Our analytic calculations agree with the results of population synthesis studies. In addition, we extend our calculations to planets in the super-Earth mass range.

2 LIDOV-KOZAI OSCILLATIONS WITH OCTUPOLE EFFECT AND SHORT-RANGE FORCES: MAXIMUM ECCENTRICITY

The success of LK migration depends on the maximum eccentricity e_{max} that can be achieved by the planet in the LK cycles. This eccentricity needs to be high enough such that the pericenter separation between the planet and its host star is sufficiently small for tidal dissipation in the planet to be efficient (see Section 3.1). The maximum eccentricity depends on the initial inclination i_0 between the planetary and binary orbital axes, and on various system parameters: a_0 (initial planetary semi-major axis), a_{out} and e_{out} (binary

semi-major axis and eccentricity), M_p , M_* , M_{out} (masses of the planet, host star and outer binary companion), and the planet’s radius R_p and its internal structure (Love number).

In Liu, Muñoz & Lai (2015) (hereafter LML), we have studied the maximum eccentricity in LK oscillations including the octupole potential of the binary companion and the effect of short-range forces (associated with General Relativity, the tidal bulge and rotational bulge of the planet). Here we summarize the key results needed for this paper.

The strength of the octupole potential from the binary companion relative to the quadrupole potential is characterized by the dimensionless ratio

$$\epsilon_{\text{Oct}} \equiv \frac{a_0}{a_{\text{out}}} \frac{e_{\text{out}}}{1 - e_{\text{out}}^2}. \quad (2)$$

When $\epsilon_{\text{Oct}} \rightarrow 0$, the octupole effect can be neglected. In this limit, the planet’s dimensionless angular momentum (projected along the binary axis) $j_z = \sqrt{1 - e^2} \cos i$ is conserved, resulting in regular LK oscillations in eccentricity and inclination. Together with the conservation of energy, the maximum eccentricity e_{max} can be calculated analytically as a function of i_0 (and other parameters) (Fabrycky & Tremaine 2007). Assuming that the planet has zero initial eccentricity, e_{max} is determined by (LML)

$$\epsilon_{\text{GR}} \left(\frac{1}{j_{\text{min}}} - 1 \right) + \frac{\epsilon_{\text{Tide}}}{15} \left(\frac{1 + 3e_{\text{max}}^2 + \frac{3}{8}e_{\text{max}}^4}{j_{\text{min}}^9} - 1 \right) + \frac{\epsilon_{\text{Rot}}}{3} \left(\frac{1}{j_{\text{min}}^3} - 1 \right) = \frac{9}{8} \frac{e_{\text{max}}^2}{j_{\text{min}}^2} \left(j_{\text{min}}^2 - \frac{5}{3} \cos^2 i_0 \right), \quad (3)$$

where $j_{\text{min}} \equiv \sqrt{1 - e_{\text{max}}^2}$, and the dimensionless quantities

$$\epsilon_{\text{GR}} \equiv \frac{3GM_*^2 a_{\text{out}}^3 (1 - e_{\text{out}}^2)^{3/2}}{a_0^4 c^2 M_{\text{out}}} \quad (4a)$$

$$\epsilon_{\text{Tide}} \equiv \frac{15M_*^2 a_{\text{out}}^3 (1 - e_{\text{out}}^2)^{3/2} k_{2p} R_p^5}{a_0^8 M_p M_{\text{out}}} \quad (4b)$$

$$\epsilon_{\text{Rot}} \equiv \frac{M_* a_{\text{out}}^3 (1 - e_{\text{out}}^2)^{3/2} k_{qp} \Omega_p^2 R_p^5}{G a_0^5 M_p M_{\text{out}}}, \quad (4c)$$

represent the relative strengths of apsidal precessions due to General Relativity (GR), tidal bulge, and rotational distortion of the planet. Here k_{2p} is the Love number, k_{qp} the apsidal motion constant and Ω_p the rotation rate of the planet. In the “pure” LK limit ($\epsilon_{\text{GR}} = \epsilon_{\text{Tide}} = \epsilon_{\text{Rot}} = 0$), Equation (3) reduces to the standard expression $e_{\text{max}} = \sqrt{1 - (5/3) \cos^2 i_0}$. For typical planetary rotation rates, the contribution from the rotational bulge (ϵ_{Rot}) can be neglected compared to the tidal term (ϵ_{Tide}) (see LML).

The maximum value of e_{max} is achieved when $i_0 = 90^\circ$ in Equation (3), and is referred to as the “limiting eccentricity” e_{lim} . When $e_{\text{lim}} \approx 1$, the limiting eccentricity satisfies (Eq. 53 of LML)

$$\frac{\epsilon_{\text{GR}}}{(1 - e_{\text{lim}}^2)^{1/2}} + \frac{7}{24} \frac{\epsilon_{\text{Tide}}}{(1 - e_{\text{lim}}^2)^{9/2}} \simeq \frac{9}{8}. \quad (5)$$

In the presence of finite octupole potential ($\epsilon_{\text{Oct}} \neq 0$), j_z is no longer a constant, but a slowly varying quantity (Ford, Kozinsky & Rasio 2000; Lithwick & Naoz 2011; Katz, Dong & Malhotra 2011), with $dj_z/dt \propto \epsilon_{\text{Oct}}$. For sufficiently large initial inclinations ($i_0 > i_{\text{lim}}$), the slow evolution of j_z can take it to extremely small values and even make it cross zero (i.e. $i \rightarrow 90^\circ$, see e.g., Katz, Dong & Malhotra 2011). As j_z becomes small, e can reach very high values.

As described by LML, the effect of the octupole is to increase the range of possible initial angles i_0 for which e_{lim} can be reached. To capture the effect described by LML, we can approximate the

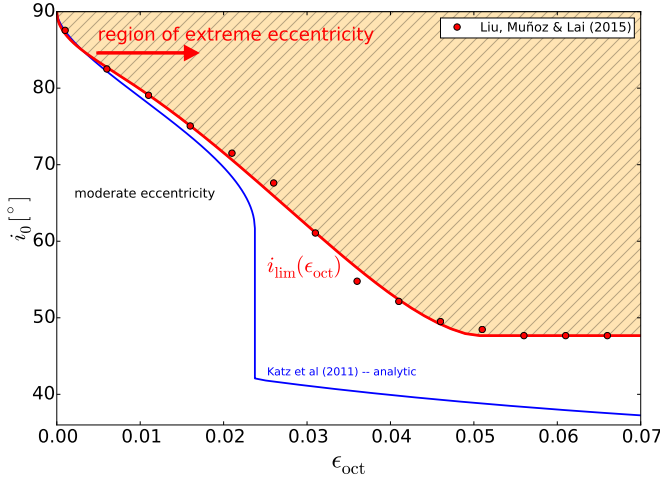


Figure 1. The behavior of LK oscillations with the octupole and short-range-force (SRF) effects can be divided into “moderate” eccentricity evolution and “extreme” eccentricity evolution. The boundary between these two regions is a function of ϵ_{Oct} (the dimensionless octupole strength) and i_0 (the initial inclination). In the $\epsilon_{\text{Oct}}-i_0$ plane, this boundary is represented by the critical initial angle $i_{\text{lim}}(\epsilon_{\text{Oct}})$ above which planets can reach the limiting eccentricity e_{lim} (Equation 5). The data points are taken from the numerical integrations of Liu, Muñoz & Lai (2015) and the red curve depicts the fitting function (Equation 7). For $\epsilon_{\text{Oct}} \gtrsim 0.05$, $i_{\text{lim}}(\epsilon_{\text{Oct}})$ flattens out to a constant value $\approx 48^\circ$. For comparison, the blue curve shows the analytic result for the critical i_0 for orbital flip without SRF, as obtained by Katz, Dong & Malhotra (2011).

maximum eccentricity with ²

$$e_{\text{max}}(i_0, \epsilon_{\text{Oct}}) \simeq \begin{cases} e_{\text{max}}^{(\text{Quad})}(i_0) & i_0 < i_{\text{lim}}(\epsilon_{\text{Oct}}) \\ e_{\text{lim}} & i_0 \geq i_{\text{lim}}(\epsilon_{\text{Oct}}) \end{cases} \quad (6)$$

where $e_{\text{max}}^{(\text{Quad})}(i_0)$ is the solution to Equation (3) and e_{lim} is the solution to Equation (5), and i_{lim} is the critical angle above which e_{lim} is reached (for $\epsilon_{\text{Oct}} \rightarrow 0$, it is required that $i_{\text{lim}} \rightarrow 90^\circ$, such that the quadrupole approximation is recovered). Note that Equation (6) neglects the “transition region” for i_0 just below i_{lim} in which the octupole potential makes e_{max} larger than $e_{\text{max}}^{(\text{Quad})}$ but not as large as e_{lim} . The numerical calculations of LML showed that when tidal distortion (ϵ_{Tide}) dominates the SRFs, the transition region is narrow.

The critical inclination angle i_{lim} , which defines the “octupole-active” window, depends on ϵ_{Oct} . Figure 1 shows the numerically computed values of i_{lim} (LML). These can be well approximated by the fitting formula

$$\cos^2 i_{\text{lim}} = A \left(\frac{\epsilon_{\text{Oct}}}{0.1} \right) + B \left(\frac{\epsilon_{\text{Oct}}}{0.1} \right)^2 + C \left(\frac{\epsilon_{\text{Oct}}}{0.1} \right)^3 + D \left(\frac{\epsilon_{\text{Oct}}}{0.1} \right)^4 \quad (7)$$

for $\epsilon_{\text{Oct}} \leq 0.05$ with $A = 0.26$, $B = -0.536$, $C = 12.05$ and $D = -16.78$. For $\epsilon_{\text{Oct}} > 0.05$, the dependence on ϵ_{Oct} flattens off at $\cos^2 i_{\text{lim}} = 0.45$ or $i_{\text{lim}} = 48^\circ$ (Fig. 1). Note that, as shown by LML, the octupole-active’ window is equivalent to the range of inclinations susceptible to orbital “flips” in LK cycles *without* SRFs. Katz, Dong & Malhotra (2011) has obtained an analytic expression

² Equation (6) is restricted to $i_0 \leq 90^\circ$. However, note that the system is symmetric around 90° , thus the limiting eccentricity is also reached for $90^\circ < i_0 < 180 - i_{\text{lim}}$.

of the critical inclination angle for orbital flip – this analytic result is valid only for $\epsilon_{\text{Oct}} \ll 1$ (see Fig. 1).

We note that, in general, the octupole-active window of extreme eccentricity is reached only when ω (the argument of pericenter) of the planet is circulating (as discussed by Katz, Dong & Malhotra 2011). However, since planets commonly start with $e \simeq 0$, this distinction is irrelevant, as planets at $e \simeq 0$ lie very close to the separatrix between the librating and circulating regions of phase space.

3 DERIVATION OF MIGRATION FRACTIONS

3.1 Required pericenter distance for migration or disruption

In order to migrate, a distant planet must reach small pericenter distance, $r_p = a_0(1 - e)$, such that tidal dissipation can reduce the planet’s semi-major axis within a few Gyr. The effective orbital decay rate during LK oscillations can be estimated from the orbital decay rate due to tidal dissipation at $e = e_{\text{max}}$ multiplied by the fraction of the time the planet spends in the high- e phase ($e \sim e_{\text{max}}$), giving (see Section 3.2 and Eq. 32 of ASL)

$$\begin{aligned} \frac{1}{t_{\text{dec}}} &\equiv \left| \frac{1}{a} \frac{da}{dt} \right|_{\text{Tide, LK}} \\ &\simeq 6k_{2p} \Delta t_L \frac{M_*}{M_p} \left(\frac{R_p}{a_0} \right)^5 n^2 \frac{f_1(e_{\text{max}})}{j_{\text{min}}^{14}} \\ &\simeq 2.8 k_{2p} \Delta t_L \frac{GM_*^2}{M_p} \frac{R_p^5}{a_0 r_{p, \text{min}}^7} \end{aligned} \quad (8)$$

where Δt is the lag time, the pericenter distance at maximum eccentricity is defined as $r_{p, \text{min}} \equiv a_0(1 - e_{\text{max}})$ and the expression $f_1(e_{\text{max}})$ is replaced by its approximate value 3861/64. In order to have migration within $\sim 10^9$ years (i.e., $t_{\text{dec}} \lesssim 10^9$ years), we require $r_{p, \text{min}} \lesssim r_{p, \text{mig}}$, with

$$\begin{aligned} r_{p, \text{mig}} &\equiv 2.4 \times 10^{-2} \left(\frac{R_p}{R_J} \right)^{\frac{5}{7}} \text{ AU} \\ &\times \left(\frac{\chi}{10} \right)^{1/7} \left(\frac{M_p}{M_J} \right)^{-1/7} \left(\frac{a_0}{1 \text{ AU}} \right)^{-1/7} \left(\frac{k_{2p}}{0.37} \right)^{1/7} \left(\frac{M_*}{1 M_\odot} \right)^{2/7}, \end{aligned} \quad (9)$$

where $\chi \equiv \Delta t/(0.1\text{s})$ is a dimensionless tidal enhancement factor.

We see that, except for planet radius, the dependence of the critical pericenter distance $r_{p, \text{mig}}$ on the physical parameters of the system is weak, and thus it represents a very robust (albeit not an exact) estimate of how close planets must get to their host stars in order to migrate effectively (see ASL). For this pericenter to be reached, a planet initially located at a_0 needs to achieve a maximum eccentricity of

$$e_{\text{mig}} \equiv 1 - \frac{r_{p, \text{mig}}}{a_0} \quad (10)$$

via LK oscillations. Note that, since the final semi-major axis a_F of the planet after tidal decay is approximately $a_F \simeq r_{p, \text{mig}}(1 + e_{\text{max}}) \simeq 2r_{p, \text{mig}}$, Equation (9) indicates that it is difficult to form HJs with $a_F \gtrsim 0.06$ AU via LK migration (Petrovich 2015b; ASL), unless the tidal dissipation parameter χ is much larger than the canonical value of 10.

Equation (9) sets the maximum pericenter separation that allows for LK migration. There is also a *minimum* pericenter separation that permits “successfully migrated” planets. For pericenter

separations smaller than the tidal radius

$$r_{p,\text{dis}} = \eta R_p \left(\frac{M_*}{M_p} \right)^{1/3} = 1.3 \times 10^{-2} \text{ AU} \left(\frac{R_p}{R_J} \right) \left(\frac{M_p}{M_J} \right)^{-1/3} \left(\frac{M_*}{M_\odot} \right)^{1/3}. \quad (11)$$

(where $\eta = 2.7$; Guillochon, Ramirez-Ruiz & Lin 2011), planets will be disrupted and therefore unable to turn into HJs. As before, for this specific pericenter to be reached, a planet initially located at a_0 needs to achieve LK maximum eccentricity of

$$e_{\text{dis}} \equiv 1 - \frac{r_{p,\text{dis}}}{a_0}. \quad (12)$$

Note that, if $r_{p,\text{dis}} > r_{p,\text{mig}}$, all migration-inducing LK oscillations will result in tidal disruptions. This condition imposes a lower limit in the planet mass that permits the formation of close-in planets:

$$M_p > 0.04 M_J \left(\frac{R_p}{R_J} \right)^{3/2} \left(\frac{\chi}{10} \right)^{-3/4} \left(\frac{M_*}{1 M_\odot} \right)^{1/4} \left(\frac{a_0}{1 \text{ AU}} \right)^{3/4} \left(\frac{k_{2p}}{0.37} \right)^{-3/4} \quad (13)$$

This implies that Saturn-mass planets can rarely migrate successfully via LK oscillations without first being disrupted (see ASL).

3.2 Migration and disruption fractions

Having defined the eccentricities required for migration and tidal disruption, we can now compute the fractions of migration and tidal disruption for given a_0 , a_{out} and e_{out} (plus the other fixed parameters of the systems such as M_p , M_* , M_{out} , R_p and χ). To achieve e_{mig} , the initial planetary inclination angle (relative to the binary) must be sufficiently large, i.e., $i_{0,\text{mig}} < i_0 < 180^\circ - i_{0,\text{mig}}$. For an isotropic distribution of the initial planetary angular momentum vectors, those that can lead to e_{mig} or larger occupy a solid angle $4\pi \cos i_{0,\text{mig}}$. Thus the migration fraction is

$$f_{\text{mig}}^{\text{LK}}(a_0, a_{\text{out}}, e_{\text{out}}) = \cos i_{0,\text{mig}}. \quad (14)$$

Similarly, the disruption fraction is given by

$$f_{\text{dis}}^{\text{LK}}(a_0, a_{\text{out}}, e_{\text{out}}) = \cos i_{0,\text{dis}}, \quad (15)$$

where $i_{0,\text{dis}}$ is the critical inclination that leads to $e_{\text{max}} = e_{\text{dis}}$. The fraction of HJ formation (migration without disruption) is simply

$$f_{\text{HJ}}^{\text{LK}}(a_0, a_{\text{out}}, e_{\text{out}}) = f_{\text{mig}}^{\text{LK}} - f_{\text{dis}}^{\text{LK}} = \cos i_{0,\text{mig}} - \cos i_{0,\text{dis}}. \quad (16)$$

3.2.1 Migration/disruption fraction in quadrupole-order theory

For $e_{\text{mig}} > e_{\text{lim}}$, no migration is possible and we have $\cos i_{0,\text{mig}} = 0$. For $e_{\text{mig}} < e_{\text{lim}}$, to quadrupole-order, the critical angle for migration $i_{0,\text{mig}}$ can be computed analytically by directly solving for $\cos i_0$ in Equation (3) with $e_{\text{max}} = e_{\text{mig}}$. Thus

$$\cos^2 i_{0,\text{mig}}^{\text{(Quad)}} = \begin{cases} C(e_{\text{mig}}) & \text{if } e_{\text{mig}} < e_{\text{lim}} \\ 0 & \text{if } e_{\text{mig}} > e_{\text{lim}} \end{cases} \quad (17)$$

where

$$C(e_{\text{mig}}) = \frac{3}{5} j_{\text{mig}}^2 - \frac{8}{15} \frac{\epsilon_{\text{GR}}}{e_{\text{mig}}^2} \left(j_{\text{mig}} - j_{\text{mig}}^2 \right) - \frac{8}{225} \frac{\epsilon_{\text{Tide}}}{e_{\text{mig}}^2} \left(\frac{1 + 3e_{\text{mig}}^2 + \frac{3}{8}e_{\text{mig}}^4}{j_{\text{mig}}^2} - j_{\text{mig}}^2 \right) \quad (18)$$

with $j_{\text{mig}} = \sqrt{1 - e_{\text{mig}}^2}$ and in which the rotational distortion effect in Equation (3) has been ignored for consistency. Note that the condition $e_{\text{mig}} < e_{\text{lim}}$ is equivalent to $C(e_{\text{mig}}) > 0$. Similarly, the critical disruption angle $i_{0,\text{dis}}^{\text{(Quad)}}$ is given by Equation (17) with e_{dis} replacing e_{mig} .

In the first panel of Fig. 2, we show $f_{\text{mig}}^{\text{LK}}$, $f_{\text{dis}}^{\text{LK}}$ and $f_{\text{HJ}}^{\text{LK}}$ for a $0.3 M_J$ planet started at different initial semi-major axis a_0 and a binary companion with $a_{\text{out}} = 200$ AU and $e_{\text{out}} = 0$. We see that, for large a_0 , SRFs are unimportant for determining e_{max} around e_{mig} , thus the shape of the curve is simply $f_{\text{mig}}^{\text{LK}} = \cos i_{0,\text{mig}} = \sqrt{3/5(1 - e_{\text{mig}}^2)} \approx \sqrt{(6/5)(r_{p,\text{mig}}/a_0)}$. For small a_0 , e_{lim} is smaller than the required e_{mig} , making the migration fraction rapidly go to zero.

3.2.2 Including the octupole effect

When the octupole effect is included ($\epsilon_{\text{Oct}} \neq 0$), the maximum eccentricity achieved in LK cycles can be approximated by Equation (6). For $e_{\text{mig}} > e_{\text{lim}}$, no migration is possible and we still have $\cos i_{0,\text{mig}} = 0$. For $e_{\text{mig}} < e_{\text{lim}}$, since a non-negligible ϵ_{Oct} can expand the range of inclination angles that produce e_{mig} , the critical angle $i_{0,\text{mig}}$ is the lowest possible angle that results in e_{mig} , i.e., $i_{0,\text{mig}} = \min(i_{0,\text{mig}}^{\text{(Quad)}}, i_{\text{lim}})$. Thus,

$$\cos^2 i_{0,\text{mig}} = \begin{cases} \max \left[C(e_{\text{mig}}), \cos^2 i_{\text{lim}}(\epsilon_{\text{Oct}}) \right], & \text{if } e_{\text{mig}} \leq e_{\text{lim}} \\ 0, & \text{if } e_{\text{mig}} > e_{\text{lim}} \end{cases} \quad (19)$$

where $C(e_{\text{mig}})$ is given by Equation (19) and $\cos^2 i_{\text{lim}}(\epsilon_{\text{Oct}})$ is given by Equation (7). An analogous expression applies to $\cos^2 i_{0,\text{dis}}$.

We illustrate the effect of the octupole term on $f_{\text{mig}}^{\text{LK}}$ and $f_{\text{dis}}^{\text{LK}}$ in the three last panels of Fig. 2. For all panels, $a_{\text{out}} \sqrt{1 - e_{\text{out}}^2} = 200$ AU, while the eccentricity is varied from 0 to 0.8. As e_{out} is increased, the value of ϵ_{Oct} for a given planet semi-major axis a_0 also grows. Going from $e_{\text{out}} = 0$ to $e_{\text{out}} = 0.8$ illustrates the gradual transition from $\cos^2 i_{0,\text{mig}} = C(e_{\text{mig}})$ for all a_0 (pure quadrupole) to $\cos^2 i_{0,\text{mig}} = \cos^2 i_{\text{lim}}(\epsilon_{\text{Oct}})$ for all a_0 (entirely dominated by the octupole effect). Note that the HJ fraction $f_{\text{HJ}}^{\text{LK}} = f_{\text{mig}}^{\text{LK}} - f_{\text{dis}}^{\text{LK}}$ is always a narrow distribution bounded by the “no-migration” limit ($e_{\text{lim}} < e_{\text{mig}}$) at small a_0 and by the tidal disruption limit ($e_{\text{max}} > e_{\text{dis}}$) at larger a_0 . The width and height of this peak is only mildly affected by the octupole contribution. On the other hand, the fraction of tidally disrupted planets $f_{\text{dis}}^{\text{LK}}$ is increased significantly for larger e_{out} . Thus, the main effect the octupole is to increase the number of disrupted planets, rather than the number of successfully migrated ones (Petrovich 2015b; ASL).

Fig. 3 shows the same examples as Fig. 2, except for a planet mass of $3 M_J$. Although the lower limit for non-zero migration is almost unchanged (see Eq. 47 of ASL), the boundary between successful migration and tidal disruption occurs at a larger a_0 (e_{dis} is larger for more massive planets, making disruption more difficult; see Equation (13). Thus, a larger fraction of these massive planets can survive LK oscillations and become HJs. The mass-dependent boundary between disruption and successful migration explains the lack of “hot Saturns” in observations (ASL). Note that, as in the previous example, the most noticeable effect of the octupole terms – which differentiate the last three panels from the first – is to increase the rate of tidal disruptions, not to significantly increase the number of HJs.

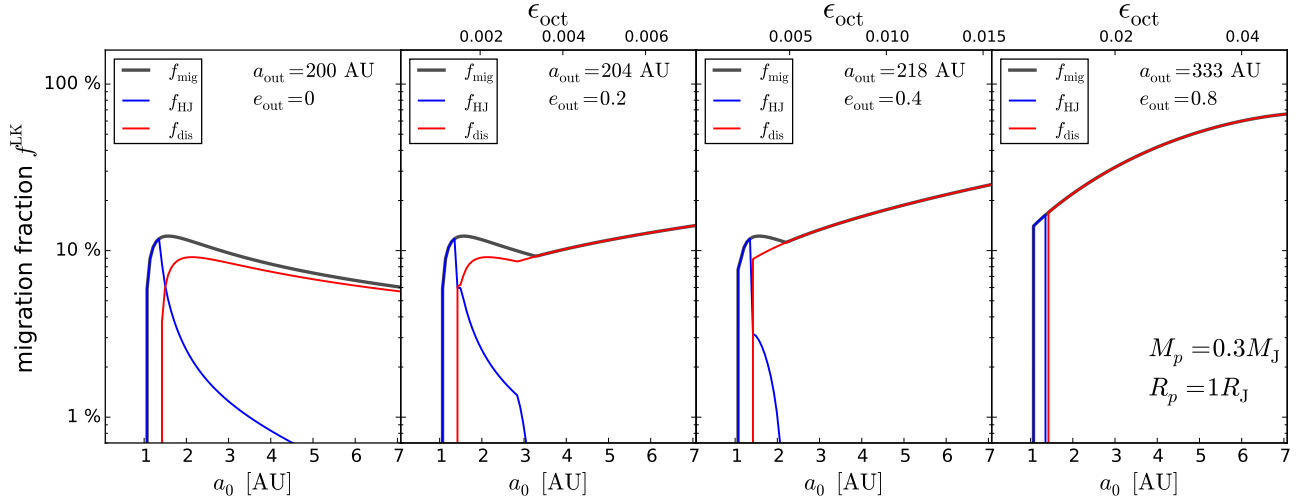


Figure 2. Migration fraction $f_{\text{mig}}^{\text{LK}}$ (Equation 14, in black), tidal disruption fraction $f_{\text{dis}}^{\text{LK}}$ (in red) and successful close-in planet formation fraction $f_{\text{HJ}}^{\text{LK}} = f_{\text{mig}}^{\text{LK}} - f_{\text{dis}}^{\text{LK}}$ (in blue) for a gas giant of mass $0.3M_J$ and tidal dissipation parameter $\chi = 10$. The first panel shows the fractions for a binary stellar companion with $a_{\text{out}} = 200$ AU and $e_{\text{out}} = 0$, for which the octupole terms in the binary potential are identically zero. The second to fourth panels show increments in e_{out} (0.2, 0.4 and 0.8) while keeping $a_{\text{out}}(1 - e_{\text{out}}^2)^{1/2}$ constant, implying a monotonic increase of the octupole strength ϵ_{Oct} . If the effects of octupole potential were neglected, all four panels would be identical. Upper horizontal axis shows ϵ_{Oct} , which is directly proportional to a_0 for fixed a_{out} and e_{out} . The main effect of the octupole potential is to increase the tidal disruption fraction. The area under the blue curve is, from left to right, 10%, 7.8%, 5.1% and 5.3%.

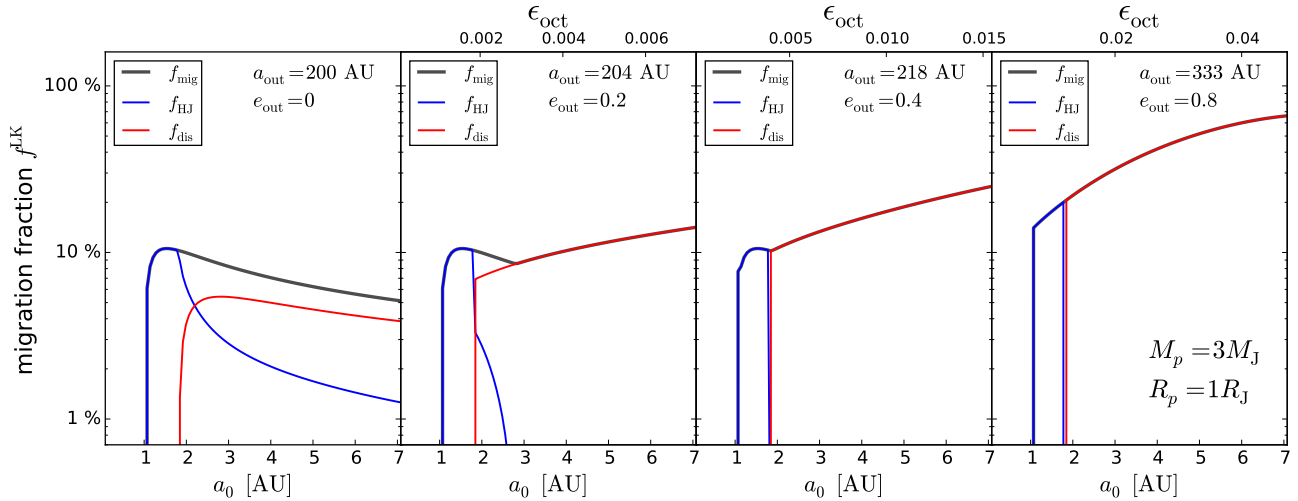


Figure 3. Same as Fig. 2 but for a planet ten times more massive ($M_p = 3M_J$). General trends are analogous to the less massive example (the total migration curve $f_{\text{mig}}^{\text{LK}}$ in black is essentially unchanged). In this case, however, planets are much more likely to survive LK migration, because the boundary between HJ formation and tidal disruption takes place at higher eccentricity (Equation 13). The area under the blue curve is, from left to right, 20%, 9.2%, 7.7% and 13%.

4 TOTAL MIGRATION FRACTIONS AS A FUNCTION OF PLANET MASS

In the previous section, we described how to calculate the migration fraction $f_{\text{mig}}^{\text{LK}}$ and disruption fraction $f_{\text{dis}}^{\text{LK}}$ for a given set of orbital parameters a_0 , a_{out} and e_{out} (Eqs. 14-15). We now consider the migration and disruption fractions integrating over a range of values in a_{out} and e_{out} :

$$F_{\text{mig}}^{\text{LK}}(a_0) = \int \int f_{\text{mig}}^{\text{LK}}(a_0, a_{\text{out}}, e_{\text{out}}) \times \frac{d^2 N}{d \log a_{\text{out}} d e_{\text{out}}} d \log a_{\text{out}} d e_{\text{out}} . \quad (20)$$

For concreteness, we adopt the integration limits of $[0, 0.8]$ for e_{out} and $[2.0, 3.0]$ for $\log_{10} a_{\text{out}}$ (ASL), although other choices are possible. We compute this integral using the Monte Carlo method, uniformly sampling e_{out} and $\log_{10} a_{\text{out}}$.

4.1 Gas giants

Fig. 4 shows $F_{\text{dis}}^{\text{LK}}(a_0)$ and $F_{\text{HJ}}^{\text{LK}}(a_0)$ for different planet masses and tidal dissipation strengths. For the fiducial dissipation parameter ($\chi = 10$), the HJ fraction of Jupiter-mass objects is 1–3% (for $a_0 = 1$ –5 AU). For Saturn-mass objects, this fraction becomes is much smaller for a wide range of a_0 . For smaller χ , the “hot

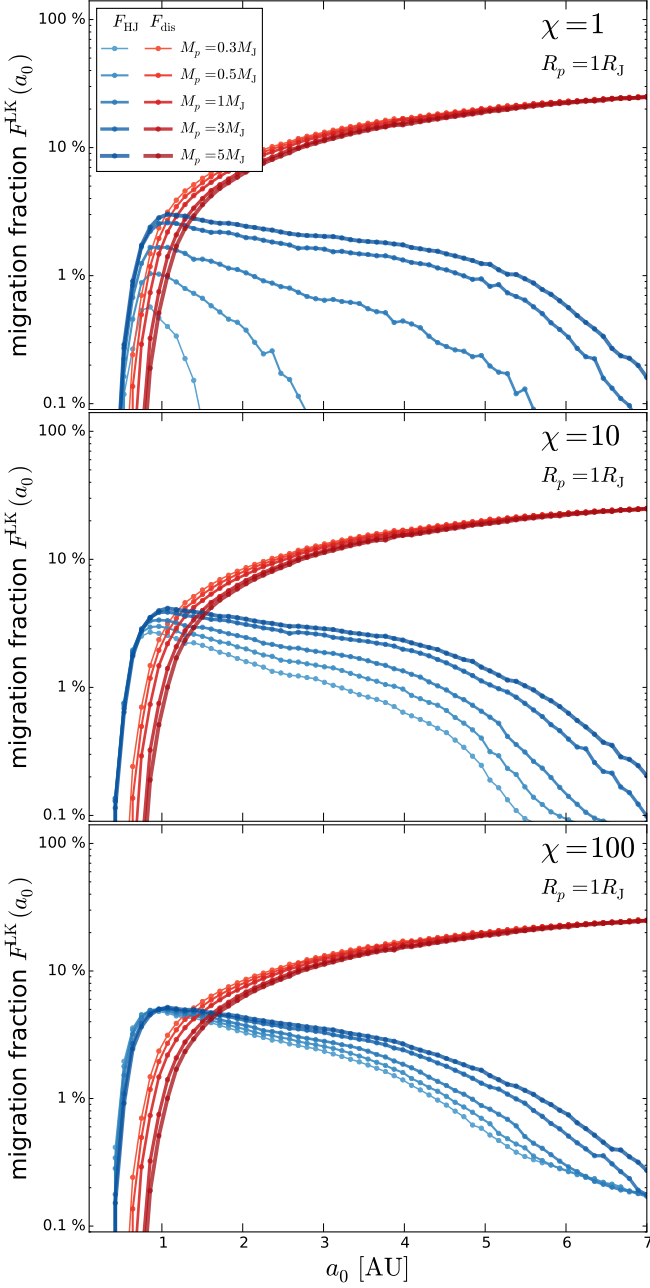


Figure 4. Integrated HJ formation fraction $F_{\text{HJ}}^{\text{LK}}(a_0)$ and tidal disruption fraction $F_{\text{dis}}^{\text{LK}}(a_0)$ (see Eq. 20) for a range of planet masses M_p and dimensionless tidal dissipation strengths χ . Planet masses are $M_p = 0.3, 0.5, 1, 3$ and $5 M_J$ and all planet radii are taken to be $R_p = R_J$. The three panels correspond to $\chi = 1, 10, 100$.

planet” fraction of Saturn-mass objects is $\ll 1\%$, while only planets with masses above $3M_J$ can successfully turn into hot planets. It is only in the extreme dissipation regime ($\chi = 100$) that all gas giants across the explored mass range can turn into hot planets at rates of a few percent. This behavior can be easily understood from the definitions of $r_{p,\text{mig}}$ and $r_{p,\text{dis}}$ (Eqs. 9 and 11). For a given χ , varying the planet mass by a factor of a few does not change significantly the total migration fraction ($F_{\text{mig}}^{\text{LK}} + F_{\text{dis}}^{\text{LK}}$) because $r_{p,\text{mig}}$ is essentially unchanged. However, the relative importance of $F_{\text{mig}}^{\text{LK}}$ and $F_{\text{dis}}^{\text{LK}}$ is changed as $r_{p,\text{dis}}$ depends on M_p . Similarly, changing

Table 1. The HJ formation fraction $\mathcal{F}_{\text{HJ}}^{\text{LK}}$, tidal disruption fraction $\mathcal{F}_{\text{dis}}^{\text{LK}}$ and total migration fraction $\mathcal{F}_{\text{mig}}^{\text{LK}}$ for gas giants with three different masses and three different dissipation strengths.

	$\chi = 1$			$\chi = 10$			$\chi = 100$		
$M_p (M_J)$	0.3	1	3	0.3	1	3	0.3	1	3
$\mathcal{F}_{\text{HJ}}^{\text{LK}} (\%)$	0	0.8	1.8	1.2	2.1	2.8	2.6	3.1	3.6
$\mathcal{F}_{\text{dis}}^{\text{LK}} (\%)$	12.4	11.6	10.8	12.4	11.6	10.8	12.4	11.6	10.8
$\mathcal{F}_{\text{mig}}^{\text{LK}} (\%)$	12.4	12.4	12.6	13.6	13.7	13.6	15	14.7	14.4

χ while keeping M_p fixed does not change $F_{\text{dis}}^{\text{LK}}$, but only $F_{\text{mig}}^{\text{LK}}$, as $r_{p,\text{mig}}$ grows slightly with stronger dissipation.

These trends are in agreement with the extensive Monte Carlo experiments of ASL. In that work, the computed total migration fractions (HJs plus tidal disruptions) depend very weakly on χ . In order to compare directly with the results of ASL, we integrate $F_{\text{mig}}^{\text{LK}}(a_0)$ over a range of planet semi-major axes. Assuming that a_0 is distributed uniformly between $a_{0,\text{inner}}$ and $a_{0,\text{outer}}$, we have:

$$\mathcal{F}_{\text{mig}}^{\text{LK}} = \int_{a_{0,\text{inner}}}^{a_{0,\text{outer}}} F_{\text{mig}}^{\text{LK}}(a_0) \frac{dN}{da_0} da_0. \quad (21)$$

Using the values $a_{0,\text{inner}} = 1$ AU and $a_{0,\text{outer}} = 5$ AU, we compute the integrated migration fractions $\mathcal{F}_{\text{mig}}^{\text{LK}}$, $\mathcal{F}_{\text{dis}}^{\text{LK}}$ and $\mathcal{F}_{\text{HJ}}^{\text{LK}}$ for three planet masses ($M_p = 0.3, 1.0$ and $3 M_J$) and three dissipation parameters ($\chi = 1, 10$ and 100). The results (see Table 1) agree with the findings of ASL. In particular, the total migration fraction is confirmed to be very robust and to lie in the range between 12% and 15%.

4.1.1 Other studies

Despite the robustness of the HJ migration fraction found by ASL, this number is not in perfect agreement with the results of other recent works, such as Naoz, Farr & Rasio (2012) and Petrovich (2015b) (both considered only $M_p = 1 M_J$). The main difference with Naoz, Farr & Rasio (2012) is in the choice of η in Equation (11). On the other hand, Petrovich (2015b) used $\eta = 2.7$, the same as ASL. However, these two last works differ in the properties of the assumed underlying population of companions (see Section 6.2 of ASL for a discussion). Here, we (and ASL) have assumed the binary orbits to follow uniform distributions in e_{out} and $\log a_{\text{out}}$, with $e_{\text{out}} \in [0, 0.8]$ and $\log a_{\text{out}} \in [2, 3]$. Following one of the examples of Petrovich (2015b), we choose $e_{\text{out}} \in [0, 0.95]$ and $\log a_{\text{out}} \in [2, 3.2]$, and find $\mathcal{F}_{\text{HJ}}^{\text{LK}} = 1.2\%$, $\mathcal{F}_{\text{dis}}^{\text{LK}} = 21.2\%$ for a total of $\mathcal{F}_{\text{mig}}^{\text{LK}} = 22.4\%$, in agreement with the results of Monte Carlo experiments.

4.2 Rocky planets

The procedure outlined in the previous section can be applied to rocky planets by simple modification of the planet mass-radius relation, Love number k_{2p} and dimensionless tidal strength χ . For Solar System rocky planets $\Delta t_L \approx 600$ s (Lambeck 1977; Neron de Surgy & Laskar 1997), i.e., $\chi = 6000$, and $k_{2p} \approx 0.3$ (Yoder 1995). We take the generic mass-radius relation from Seager et al. (2007) for an “Earth-like” composition and calculate $F_{\text{mig}}^{\text{LK}}$

and $F_{\text{dis}}^{\text{LK}}$ as above. The successful migration rate of “hot planets” is, analogous to HJs, $F_{\text{hp}}^{\text{LK}} = F_{\text{mig}}^{\text{LK}} - F_{\text{dis}}^{\text{LK}}$.

In Fig. 5, we show $F_{\text{hp}}^{\text{LK}}$ (in blue) and $F_{\text{dis}}^{\text{LK}}$ (in red) for different rocky planets, ranging in mass from $2M_{\oplus}$ to $15M_{\oplus}$. The integrated hot planet fraction $\mathcal{F}_{\text{hp}}^{\text{LK}}$ (for a_0 between 1 and 5 AU) is between 1% and 1.5%. Thus, these planets are more likely to survive LK migration than Saturn-mass planets. The reason for this is that there is enough room between $r_{p,\text{mig}}$ and $r_{p,\text{dis}}$ (Eqs. 9 and 11) to accommodate the planets into successfully migrated orbits. Rewriting $r_{p,\text{mig}}$ and $r_{p,\text{dis}}$ in units more suitable for rocky planets, we have

$$r_{p,\text{mig}} = 2.47 \times 10^{-2} \left(\frac{R_p}{1.2R_{\oplus}} \right)^{\frac{5}{7}} \text{ AU} \times \left(\frac{\chi}{6000} \right)^{1/7} \left(\frac{M_p}{2M_{\oplus}} \right)^{-1/7} \left(\frac{a_0}{1 \text{ AU}} \right)^{-1/7} \left(\frac{k_{2p}}{0.3} \right)^{1/7} \left(\frac{M_*}{1M_{\odot}} \right)^{2/7} \quad (22)$$

and

$$r_{p,\text{dis}} = 7.6 \times 10^{-3} \text{ AU} \left(\frac{R_p}{1.2R_{\oplus}} \right) \left(\frac{M_p}{2M_{\oplus}} \right)^{-1/3} \left(\frac{M_*}{1M_{\odot}} \right)^{1/3} \quad (23)$$

Interestingly, $r_{p,\text{mig}}$ is very close to the value obtained for a Jupiter-mass planet; however, $r_{p,\text{dis}}$ is smaller, since the higher density of rocky planets pushes the Roche limit closer to the star. Thus, provided χ is high enough (in this case 6000), some small but non-negligible fraction of rocky planets can survive LK oscillations and migrate into close-in orbits. Note that, for $2M_{\oplus}$ rocky planets, Eqs. (22) and (23) indicate that the LK migrated hot super-Earths should reside within an orbital period range of 0.7 to 4 days.

Note that the dimensionless tidal dissipation parameter χ is highly uncertain. Tidal dissipation in the Earth is dominated by its oceans (e.g., Peale 1999, and references therein), which does not necessarily apply to models of migrating super-Earths with uncertain amounts of gas envelopes. If we assume a smaller tidal dissipation strength ($\chi = 600$), the hot planet formation rates are reduced by a factor of two (see the caption of Fig. 5). Such small success rates in producing close-in rocky planets are in rough agreement with the N -body experiments of Plavchan, Chen & Pohl (2015), who implemented a constant-phase-lag (or constant tidal quality factor Q) model to study LK migration of small planets in the binary system α Cen B. In that study, only 1–3 integrations out of ~ 600 ended up in close-in planets.

If we write the occurrence rate of hot rocky planets formed via LK migration as (see Equation 1) $\mathcal{R}_{\text{hp}}^{\text{rocky}} = \mathcal{F}_b \times \mathcal{F}_p^{\text{rocky}} \times \mathcal{F}_{\text{hp}}^{\text{LK}}$, and assume that the planet bearing fraction of rocky planets within a few AU is $\mathcal{F}_p^{\text{rocky}} \sim 100\%$ (Petigura, Howard & Marcy 2013; Fressin et al. 2013), then, with $\mathcal{F}_b \sim 20\%$ and $\mathcal{F}_{\text{hp}}^{\text{LK}} \sim 1\%$ (see Fig. 5), we find $\mathcal{R}_{\text{hp}}^{\text{rocky}} \sim 0.2\%$. Thus, an intriguing possibility is that of LK migration playing a role in the origin of short-period rocky planets, especially for single-planet systems³. Observationally, ultra-short-period ($\lesssim 2$ days) rocky planets are found to have

³ For systems containing multiple planets with a few AU semi-major axes, LK oscillations can be suppressed by mutual planet-planet interactions if the planet mass is too large. From Eq. (7) of Muñoz & Lai (2015), the critical “shielding mass” is about $3M_{\oplus}$ for $a_0 \sim 3$ AU and a stellar companion located at 150 AU (see also Martin, Mazeh & Fabrycky 2015; Hamers, Perets & Portegies Zwart 2016). For smaller planet masses, LK oscillation may operate for each planet independently.

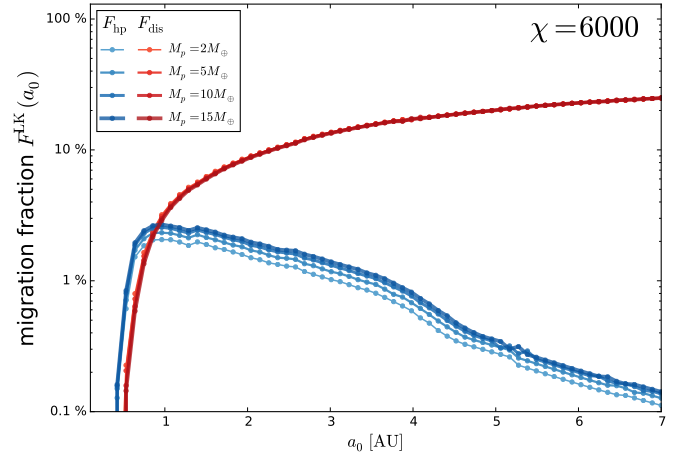


Figure 5. Integrated LK “hot planet” formation fraction $F_{\text{hp}}^{\text{LK}}(a_0)$ and tidal disruption fraction $F_{\text{dis}}^{\text{LK}}(a_0)$ as in Fig. 4 but for rocky planets. Planet masses are $M_p = 2M_{\oplus}$, $5M_{\oplus}$, $10M_{\oplus}$ and $15M_{\oplus}$, with corresponding radii of (Seager et al. 2007) $R_p = 1.2R_{\oplus}$, $1.5R_{\oplus}$, $1.8R_{\oplus}$ and $2R_{\oplus}$. When integrating $F_{\text{hp}}^{\text{LK}}(a_0)$ and $F_{\text{dis}}^{\text{LK}}(a_0)$ over a_0 between 1 and 5 AU, the global integrated fractions are, respectively, $(\mathcal{F}_{\text{hp}}^{\text{LK}}, \mathcal{F}_{\text{dis}}^{\text{LK}}) = (1.08\%, 12.9\%)$, $(1.23\%, 12.9\%)$, $(1.35\%, 12.8\%)$ and $(1.43\%, 12.7\%)$. If, instead of $\chi = 6000$ we use $\chi = 600$, the hot planet fractions are reduced by half: $(\mathcal{F}_{\text{hp}}^{\text{LK}}, \mathcal{F}_{\text{dis}}^{\text{LK}}) = (0.62\%, 12.9\%)$, $(0.74\%, 12.9\%)$, $(0.85\%, 12.8\%)$ and $(0.92\%, 12.7\%)$.

an occurrence rate of $\sim 0.5\%$ in the *Kepler* catalog (e.g. Sanchis-Ojeda et al. 2014), and the occurrence rate of rocky planets with slightly longer periods (a few days) is appreciably higher (Fressin et al. 2013). While many of these are expected to be members of multiple-planet systems (Sanchis-Ojeda et al. 2014), some may be true “singles” (Steffen & Farr 2013). LK migration of rocky planets may contribute to this population of close-in planets.

5 SUMMARY

We have derived a simple analytical method for calculating migration fractions of close-in planets via Lidov-Kozai oscillations in stellar binaries. An important ingredient of the method is the relationship between the maximum eccentricity e_{max} that can be achieved in LK oscillations as a function of the initial planet-binary inclination (Equation 6) – the effects of short-range forces and octupole potential play an essential role. Our method can be easily implemented for various planet and stellar/companion types, and consists of the following steps:

- For given initial planet semi-major axis a_0 and binary orbital parameters (a_{out} and e_{out}), calculate the “migration eccentricity” $e_{\text{mig}} = 1 - r_{p,\text{mig}}/a_0$, with $r_{p,\text{mig}}$ (the required pericenter distance in order for tidal dissipation to induce efficient orbital decay) given by Equation (9).
- Knowing e_{mig} and the octupole parameter ϵ_{oct} , calculate the critical planet-binary inclination angle for migration, $i_{0,\text{mig}}$, using Equation (19).
- Assuming isotropic distribution of the binary orientations, the migration fraction is $f_{\text{mig}}^{\text{LK}} = \cos i_{0,\text{mig}}$. The tidal disruption fraction is similarly calculated from $f_{\text{dis}}^{\text{LK}} = \cos i_{0,\text{dis}}$ and the HJ (hot planet) formation fraction is $f_{\text{HJ}}^{\text{LK}} = f_{\text{mig}}^{\text{LK}} - f_{\text{dis}}^{\text{LK}}$.
- For a distribution of a_0 , a_{out} and e_{out} , the integrated migration/disruption fractions can be obtained using Eqs. 20 and 21.

The results of our calculations are in good agreement with the recent population studies of HJ formation via LK migration in stellar binaries (Petrovich 2015b; Anderson, Storch & Lai 2016). They can be easily modified to reflect different types of planets/binaries and distributions of the binary's orbital elements. This agreement confirms that the total migration fraction of planets (the sum of HJ and tidal disruption fractions) via the LK mechanism is primarily determined by the initial geometry of the hierarchical triple, and depends weakly on the properties of the planet (Anderson, Storch & Lai 2016). The production fraction of close-in planets, on the other hand, does depend on the internal properties of the planet (e.g., mass-radius relation and the strength of dissipation), and it decreases with decreasing mass in the case of gas giants, resulting in a natural absence of “hot Saturns”. In addition, we find that rocky planets, provided they are sufficiently dissipative, may migrate more effectively than Saturn-mass planets. It is possible that some fraction of the observed short-period rocky planets are produced via LK migration in stellar binaries.

ACKNOWLEDGEMENTS

We thank Kassandra Anderson for useful discussions and Cristóbal Petrovich for comments on the manuscript. This work has been supported in part by NSF grant AST-1211061, and NASA grants NNX14AG94G and NNX14AP31G.

REFERENCES

- Anderson K. R., Storch N. I., Lai D., 2016 (ASL), *MNRAS*, 456, 3671
- Beaugé C., Nesvorný D., 2012, *ApJ*, 751, 119
- Chatterjee S., Ford E. B., Matsumura S., Rasio F. A., 2008, *ApJ*, 686, 580
- Correia A. C. M., Laskar J., Farago F., Boué G., 2011, *Celestial Mechanics and Dynamical Astronomy*, 111, 105
- Dawson R. I., Murray-Clay R. A., 2013, *ApJ*, 767, L24
- Dawson R. I., Murray-Clay R. A., Johnson J. A., 2015, *ApJ*, 798, 66
- Fabrycky D., Tremaine S., 2007, *ApJ*, 669, 1298
- Ford E. B., Kozinsky B., Rasio F. A., 2000, *ApJ*, 535, 385
- Fressin F. et al., 2013, *ApJ*, 766, 81
- Goldreich P., Tremaine S., 1980, *ApJ*, 241, 425
- Guillochon J., Ramirez-Ruiz E., Lin D., 2011, *ApJ*, 732, 74
- Hamers A. S., Perets H. B., Portegies Zwart S. F., 2016, *MNRAS*, 455, 3180
- Howard A. W. et al., 2012, *ApJS*, 201, 15
- Jurić M., Tremaine S., 2008, *ApJ*, 686, 603
- Katz B., Dong S., Malhotra R., 2011, *Physical Review Letters*, 107, 181101
- Kozai Y., 1962, *AJ*, 67, 591
- Lambeck K., 1977, *Philosophical Transactions of the Royal Society of London Series A*, 287, 545
- Lidov M. L., 1962, *P&SS*, 9, 719
- Lin D. N. C., Bodenheimer P., Richardson D. C., 1996, *Nature*, 380, 606
- Lithwick Y., Naoz S., 2011, *ApJ*, 742, 94
- Liu B., Muñoz D. J., Lai D., 2015 (LML), *MNRAS*, 447, 751
- Marcy G., Butler R. P., Fischer D., Vogt S., Wright J. T., Tinney C. G., Jones H. R. A., 2005, *Progress of Theoretical Physics Supplement*, 158, 24
- Martin D. V., Mazeh T., Fabrycky D. C., 2015, *MNRAS*, 453, 3554
- Muñoz D. J., Lai D., 2015, *Proceedings of the National Academy of Science*, 112, 9264
- Nagasawa M., Ida S., Bessho T., 2008, *ApJ*, 678, 498
- Naoz S., Farr W. M., Rasio F. A., 2012, *ApJ*, 754, L36
- Neron de Surgy O., Laskar J., 1997, *A & A*, 318, 975
- Peale S. J., 1999, *ARA&A*, 37, 533
- Petigura E. A., Howard A. W., Marcy G. W., 2013, *Proceedings of the National Academy of Science*, 110, 19273
- Petrovich C., 2015a, *ApJ*, 805, 75
- Petrovich C., 2015b, *ApJ*, 799, 27
- Plavchan P., Chen X., Pohl G., 2015, *ApJ*, 805, 174
- Raghavan D. et al., 2010, *ApJS*, 190, 1
- Rasio F. A., Ford E. B., 1996, *Science*, 274, 954
- Sanchis-Ojeda R., Rappaport S., Winn J. N., Kotson M. C., Levine A., El Mellah I., 2014, *ApJ*, 787, 47
- Seager S., Kuchner M., Hier-Majumder C. A., Militzer B., 2007, *ApJ*, 669, 1279
- Steffen J. H., Farr W. M., 2013, *ApJ*, 774, L12
- Storch N. I., Anderson K. R., Lai D., 2014, *Science*, 345, 1317, preprint(arXiv:1409.3247)
- Wright J. T., Marcy G. W., Howard A. W., Johnson J. A., Morton T. D., Fischer D. A., 2012, *ApJ*, 753, 160
- Wu Y., Lithwick Y., 2011, *ApJ*, 735, 109
- Wu Y., Murray N., 2003, *ApJ*, 589, 605
- Wu Y., Murray N. W., Ramsahai J. M., 2007, *ApJ*, 670, 820
- Yoder C. F., 1995, in *Global Earth Physics: A Handbook of Physical Constants*, Ahrens T. J., ed., p. 1